IRAQI STATISTICIANS JOURNAL

https://isj.edu.iq/index.php/isj

ISSN: 3007-1658 (Online)

Deep Functional Median Polish: A Robust Framework Integrating Functional Depth and Median-Based Decomposition for Long-Term Financial Time Series

Abdulsalam M. Sabri[1], and Qasim N. Husain[2]

[1] Department of mathematics, College of Computer Science and mathematics, Tikrit University, 34001 Baghdad, Iraq.
[,2] Mathematics Departments, Education for Pure Science College, Tikrit University, 34001 Baghdad, Iraq.

ARTICLE INFO

Article history:
Received
Revised
Accepted
Available online

Keywords:
Functional Data Analysis
Functional Median Polish
Deep Functional Median Polish
Financial Time Series
Seasonal Decomposition
Robust Functional Modeling

ABSTRACT

This research builds upon the successive development of robust functional analysis methods, starting with the Median Polish (MP) algorithm, which provided a powerful additional model for handling bidirectional data, progressing through Functional Median Polish (FMP), and culminating in the integration of functional depth measures into a single framework. This work presents a new framework called Deep Functional Median Polish (Deep FMP), which combines the robustness of median statistics in the MP algorithm with the inherent geometric properties of functional depth measures to characterize the hierarchical structure of complex functional time series. Also applies the proposed model to financial data spanning 34 years, comprising 408 views structured in a 34×12 matrix. Each year is transformed into a smoothed function using Fourier's rule, and then PCA is used to derive a highly interpreted latent space, where the first component explains 94.3% of the total variance. Subsequently, the median model is applied to the latent space to separate the general, annual, seasonal, and residual components. The results demonstrated a high capacity for accurately reconstructing time-related behaviour, with near-normal residuals centred around 0.65, and a clear seasonal distribution that increases in January and December and decreases in the middle of the year.

The results prove that combining depth measures with Median Polish provides high explanatory power and enhances the model's resistance to outliers, with clear applicability to economic data with complex time-related patterns. This model opens the way for future applications in forecasting, risk analysis, and detecting structural shifts in long-term functional data.

1. Introduction

Over the past five decades, data analysis has undergone a profound evolution, moving from classical exploratory methods to robust and advanced functional approaches. This evolution can be traced back to Tukey's seminal 1977 work, which introduced the concept of Exploratory Data Analysis and proposed the Median Polish (MP) algorithm as a robust additive model capable of analyzing two-way tables and decomposing them into key components, including the overall effect, row effect, column effect, and residual errors [17]. Later studies, such as Husain et al. (2016), extended Tukey's original smoothing and additive modeling principles to modern computational contexts, broadening their applicability to diverse data structures [6]. This foundational work established the cornerstone for handling noisy or heterogeneous data without the need for strict distributional assumptions.

Since then, the Median Polish algorithm has experienced significant expansion in its

* Abdulsalam M. Sabri
E-**mail** address: am230036pcm@st.tu.edu.iq

applications to more complex data structures. Berke (2001) integrated it with Kriging in what became known as Modified Median Polish Kriging for analyzing spatiotemporal environmental data [2]. Jayaram and Klawonn (2012), and later Klawonn et al. (2013), enhanced the model's capabilities through the introduction of additive generators and power transformations, making it applicable to nonlinear and non-additive data [7][9]. Ajoge (2017) demonstrated the applicability of MP in the analysis of paired medical data, emphasizing its robustness and interpretability [1].

With the emergence of Functional Data Analysis (FDA) which treats observations as continuous functions or curves rather than discrete points the need arose to extend MP to functional data. Sun and Genton (2012) introduced the Functional Median Polish (FMP) model, reformulating the MP algorithm to suit functional data, thereby enabling the decomposition of data into continuous functional components and the precise identification of temporal and structural effects [16]. Subsequently, Qu et al. (2021) developed a robust framework for Functional Multivariate Analysis of Variance (Robust Functional MANOVA) based on FMP, demonstrating its effectiveness in analyzing complex multivariate environmental data [13]. Sun, Chen, and Genton (2012) also provided a comprehensive review that positioned FMP within the broader framework of Robust Functional Data Analysis, confirming its flexibility and computational efficiency [16].

In parallel with the development of FMP, the concept of data depth emerged as a powerful tool for ranking observations and quantifying their centrality within functional distributions. Zuo (2003) and López-Pintado & Romo (2009) established the theoretical foundations of Functional Depth, defining it as a measure of how centrally a function lies within a dataset [10][18]. These ideas were further extended through the Total Variation Depth proposed by Huang & Sun (2016) [5], the Local Depth by Sguera et al. (2016) [15], and the depth based estimation approach in functional autoregressive models (Martínez-Hernández et al., 2019) [12]. Collectively, these developments enhanced the ability of functional data analysis to resist outliers and accurately identify central functional patterns.

In recent years, research has advanced toward integrated and quantile based depth metrics that combine robust statistics and functional geometry. Luo et al. (2025) proposed the Quantile Integrated Depth metric to address noisy functional data [11], while Elías & Nagy (2025) investigated the statistical properties of integrated depth measures in incomplete data [4]. Dammer et al. (2023) developed the TAMPOR model—based on a tunable median polish approach for harmonizing high-dimensional omics data [3]. Additionally, Rigueira et al. (2025) integrated multivariate functional analysis with machine learning techniques to detect anomalies in sensor data [14]. Recent works, such as Jiménez Varón (2024), have also explored visualization, characterization, and forecasting in multivariate and functional time series, reinforcing the trend toward integrated and intelligent analytical frameworks [8].

These advancements represent the modern direction of combining depth, robustness, and artificial intelligence into a unified analytical paradigm. This evolutionary progression from the classical Median Polish (Tukey, 1977), through its functional adaptation (Sun & Genton, 2012), to the integrated Functional Depth models (López-Pintado & Romo, 2009; Luo et al., 2025) paves the way for the development of a new framework termed Deep Functional Median Polish (Deep FMP), which merges the robustness of Median Polish with the descriptive power of depth measures to characterize the hierarchical structure of functional data.

Despite advancements in robust functional analysis methods, previous studies have largely treated Median Polish and Functional Depth as separate methodologies. A unified framework that integrates both concepts to represent the multilayered structure of functional data has yet to be proposed. This gap underscores the need to develop a Deep Functional Median Polish model that fuses statistical robustness

(via the median) with geometric structure (via depth).

The significance of this study lies in its contribution to advancing robust functional analysis by integrating the two fundamental components of contemporary statistics: the median, as a measure of robustness against outliers, and depth, as a geometric framework for organizing functional data in high-dimensional, nonlinear spaces. This integration enhances modeling accuracy and interpretability in highly complex and volatile domains such as financial, environmental, and sensor data.

This research aims to develop an integrated statistical framework, termed Deep Functional Median Polish (Deep FMP), which combines statistical robustness and functional depth within the functional decomposition of data. The goal of this framework is to build a model that can more effectively and interpretively depict structural and temporal relationships in functional data.

This study has the following particular aims:

1. Developing a Deep Functional Median Polish model integrating depth measurements inside the functional data decomposition, hence enhancing the representation of hierarchical structure and temporal features in functions.
2. Using long-term functional financial data (e.g., monthly exchange rate data), to assess the performance of the suggested model in terms of interpretability and robustness.
3. Assess the outcomes of the suggested model against those of traditional techniques including Robust Functional Data Analysis (RFDA) and Functional Median Polish (FMP) to compare their usefulness in identifying temporal changes, seasonal patterns, and outliers in functional data.

2. Deep function Median Polish (PFMP)

The methodology for this technique given by steps:

1) Formulating the plural functional model and identifying constraints.
2) Details of the basis, its selection criteria, and smoothing, if applicable.
3) Basis choice and smoothing (Fourier or spline with P,λ and GCV).
4) PCA or FPCA construction and PVE criteria.
5) Median-polish algorithm (including weighted version if used).
6) Median smoothing algorithm and number of cycles.
7) Bootstrap uncertainty procedures.
8) Performing S_G, S_C, S_R, S_E strength measures and residual diagnostics.

Mathematically

1. Let $Y = \{y_{ij}\}$, where $i = 1, \dots, R$ represents years (rows), and $j = 1, \dots, C$ represents months (columns, usually $C = 12$). Each observation y_{ij} corresponds to one month in one year. We want to decompose the functional form of each time series into the following additive model:
   $x_{ij}(t) = G(t) + R_i(t) + C_j(t) + \epsilon_{ij}(t)$
   where G(t) is the overall functional trend (global effect), $R_i(t)$ is the row effect (yearly deviation), $C_j(t)$ is the column effect (monthly or seasonal deviation), $\epsilon_{ij}(t)$ is the residual component.
2. Each row $\boldsymbol{i}$ (a year) is treated as a continuous function $\boldsymbol{x_i(t)}$ defined on the interval [1, 12]. We approximate it using a Fourier basis with p basis functions:
   $B(t) = \left[B_1(t), B_2(t), \dots, B_p(t)\right]^T$ (1)
   The basis functions are defined as:
   $B_1(t) = 1, B_{2k}(t) = \sin\left(\frac{2\pi kt}{C}\right) B_{2k+1}(t) = \cos\left(\frac{2\pi kt}{C}\right)$.
   Then, each row is approximated as
   $$x_i(t) \approx B(t)^T * c_i = \sum_{m=1}^{P} B_m(t) c_{im} \quad (2)$$
   , and the coefficient vector c_i is estimated by least squares:
   $$\hat{c}_i = \arg\min_{C} \sum_{j=1}^{C} \left(x_{ij} - B\left(t_j\right)^T c\right)^2 \quad (3)$$
   This formulation seeks the coefficient vector c that minimizes the sum of squared

differences between the observed data x_{ij} and the fitted functional model $B(t_j)^T c$, where $B(t_j)$ represents the vector of basis functions evaluated at point t_j. In closed form, the least squares solution is given by:

$$\hat{c}_i = (B^T B)^{-1} B^T x_i \quad (4)$$

Here B is the design matrix containing basis function values, x_i is the vector of observed data for the i^{th} function, $\hat{c}_i$ is the estimated coefficient vector that best approximates x_i in the least squares sense as $c_i \in \mathbb{R}^p$.

3. After estimating the coefficient vector for each year, we form the coefficient matrix:

$$\boldsymbol{C} = \begin{bmatrix} \boldsymbol{c_1^T} \\ \boldsymbol{c_2^T} \\ \vdots \\ \boldsymbol{c_R^T} \end{bmatrix} \in \mathbb{R}^{\boldsymbol{R \times p}}$$

This matrix represents the smoothed functional form for each year in the basis coefficient space, where each row corresponds to one year and each column corresponds to one basis function coefficient.

4. To analyze both year (**i**) and month (**j**) effects simultaneously, each coefficient vector $\hat{\mathbf{c}}_\mathbf{i}$ is replicated across all months **j**.

$$\boldsymbol{C_{ij} = \hat{c}_i, \ \forall j}$$

This produces a three-dimensional structure, where each cell $(\boldsymbol{i, j})$ corresponds to a specific year–month combination. Then, this 3D array is reshaped into a flat matrix:

$$\boldsymbol{C_{mat}} \in \mathbb{R}^{\boldsymbol{N \times p}}, \ \boldsymbol{N = R \times C}$$

Each row of $\boldsymbol{C_{mat}}$ represents one specific time cell $(\boldsymbol{i, j})$ in the dataset.

5. Weighting using Functional Depth by Compute the Fraiman–Muniz functional depth for each curve $\mathbf{x_i(t)}$:

$$\boldsymbol{D_{FM} = 1 - \frac{1}{C}\sum_{j=1}^{C} \left| F_{t_j}\left(x_i(t_j)\right) - 0.5 \right|} \quad (5)$$

where $\boldsymbol{F_{t_j}\left(x_i(t_j)\right)}$ is the empirical cumulative distribution function evaluated at time $\boldsymbol{t_j}$.

After normalization to the range [0,1], robust weights are obtained as:

$$\boldsymbol{w_i = \frac{D_{FM}}{\max D_{FM}}}, \qquad \boldsymbol{\sum w_i = 1} \quad (6)$$

These weights $\boldsymbol{w_i}$ are then replicated across columns to obtain:

$$\boldsymbol{w_{ij} = w_i}$$

This ensures that each temporal cell $(\boldsymbol{i, j})$ inherits the same weight as its corresponding year, maintaining consistency in the weighting across months.

6. Principal Component Analysis (PCA) perform PCA on the coefficient matrix to reduce dimensionality and capture the dominant patterns of variation:

$$\boldsymbol{S = \frac{1}{N-1}(C_{mat} - \mu)^T (C_{mat} - \mu)} \quad (7)$$

where $\boldsymbol{S}$ is the covariance matrix, $\boldsymbol{\mu}$ is the mean vector across all rows.

Extract eigenvectors and eigenvalues:

$$\boldsymbol{SV = V diag(\lambda_1, \dots, \lambda_p)} \quad (8)$$

contains the eigenvalues representing the variance explained by each principal component. Retain the first $\boldsymbol{k}$ eigenvectors (columns of $\boldsymbol{V}$) corresponding to the largest eigenvalues these represent the most significant components of variation. The coordinates of each time cell in the latent space are computed as:

$$\boldsymbol{Z = (C_{mat} - \mu) V_k}$$

The percentage of variance explained (PVE) by each component is:

$$\boldsymbol{PVE_l = 100 \times \frac{\lambda_l}{\sum_m \lambda_m}} \quad (9)$$

7. Constructing the Latent Space Matrix by reshape the PCA-transformed matrix $\boldsymbol{Z}$ into a 3D tensor:

$$\boldsymbol{Z_{ij}(l), \qquad i = 1, \dots, R; \ j = 1, \dots, C; \ l = 1, \dots, k}$$

Each layer $\boldsymbol{l}$ represents a latent component capturing distinct structural variation across years and months.

8. Apply Median Polish Algorithm (Tukey's Median Polish), a robust method for additive decomposition of two-way tables, to each latent layer $\boldsymbol{Z_{ij}(l)}$:

$$Z_{ij}(l) = m(l) + r_i(l) + c_j(l) + e_{ij}(l) \quad (10)$$

Iteration steps:

i. Compute row medians: $r_i(l) = median_j\left(Z_{ij}(l)\right)$
Then subtract row medians from the data: $Z_{ij}(l) \rightarrow Z_{ij}(l) - r_i(l)$

ii. Compute column medians: $c_j(l) = median_i\left(Z_{ij}(l)\right)$
Then subtract row medians from the data: $Z_{ij}(l) \rightarrow Z_{ij}(l) - c_j(l)$

iii. Compute overall median: $m(l) = median_{i,j}\left(Z_{ij}(l)\right)$
Then subtract row medians from the data: $Z_{ij}(l) \rightarrow Z_{ij}(l) - m(l)$

These steps are repeated for a predefined number of iterations to ensure convergence. The outputs are: $m(l), r_i(l), c_j(l), e_{ij}(l)$.

9. After median polishing, the latent structure can be written as:

$$Z_{ij}(l) = \underbrace{m(l)}_{Global\ trend} + \underbrace{r_i(l)}_{Row\ effect} + \underbrace{c_j(l)}_{Column\ effect} + \underbrace{e_{ij}(l)}_{Residuals} \quad (11)$$

Then reconstruct each cell as a sum of its components:

$$Z_{ij}(l) = Z_{ij}^{center} + Z_{ij}^{row} + Z_{ij}^{col} + Z_{ij}^{res} \quad (12)$$

10. For each cell (i, j), the reconstructed coefficient vector is obtained by projecting back into the basis space:

$$c_{ij}^{(.)} = \mu + V_k Z_{ij}^{(.)}, \ (.) \in \{center, row, colomn, residuals\}$$

Each part corresponds to a distinct functional component (global, yearly, monthly, and residual).

11. Finally, each functional component is mapped back to the time domain using the basis matrix $B(t)$:

$$X_{ij}^{(.)}(t) = B(t)^T c_{ij}^{(.)} \quad (13)$$

Thus, the full reconstructed time series for each cell is:

$$X_{ij}(t) = X_{ij}^{center}(t) + X_{ij}^{row}(t) + X_{ij}^{col}(t) + X_{ij}^{res}(t) \quad (14)$$

This yields a complete functional decomposition, separating global trends, inter-annual variations, intra-annual (seasonal) effects, and residual fluctuations.

12. Extraction of Global Components by compute the average across the entire grid to extract the main structural components of the functional data. Then the global component (trend), row component (yearly variation), column component (monthly seasonality), Residual component can be founded respectively:

$$G(t) = \frac{1}{RC}\sum_{i,j} X_{ij}^{center}(t) \quad (15)$$

$$R_i(t) = \frac{1}{C}\sum_{i,j} X_{ij}^{row}(t) \quad (16)$$

$$C_j(t) = \frac{1}{R}\sum_{i,j} X_{ij}^{col}(t) \quad (17)$$

$$e_{ij}(t) = X_{ij}^{res}(t) \quad (18)$$

where $G(t)$ represents the central, long-term trend of the series the smooth average evolution of the data over time, $R_i(t)$ shows structural differences between years, identifying how specific years deviate upward or downward from the overall trend, $C_j(t)$ Reveals the monthly or seasonal effected escribing the repeated intra-year fluctuations that form the cyclical pattern, and $e_{ij}(t)$ Captures noise or residual dynamics that are not explained by the trend or seasonal structure. These may correspond to anomalies, shocks, or temporary irregularities.
This represents the unexplained fluctuations or local irregularities in the functional structure.

13. Find The cumulative variance explained up to component k is:

$$cum(PVE_k) = \sum_{l=1}^{k} PVE_l \quad (19)$$

A suitable choice of k satisfies $cum(PVE_k) \geq 90\%$, this ensures that the selected components capture most of the total variability in the dataset.

14. To maintain clear separation among the additive components and avoid overlap

between effects, the following identification conditions are imposed:

$$\sum_{i=1}^{R} \boldsymbol{R_i(t)} = \mathbf{0}, \sum_{j=1}^{C} \boldsymbol{C_j(t)} = \mathbf{0}, \boldsymbol{median_{i,j}}\left(\boldsymbol{e_{ij}(t)}\right) = \mathbf{0}$$

Together, these ensure that each extracted component represents a distinct, non-overlapping part of the total signal allowing clear interpretation of trend, yearly, seasonal, and residual dynamics.

15. Find Depth-weighted PCA covariance by equation:

$$\boldsymbol{S_w} = \frac{\mathbf{1}}{\sum_{n=1}^{N} \boldsymbol{w_n}} \sum_{n=1}^{N} \boldsymbol{w_n}(\boldsymbol{C_{mat}} - \boldsymbol{\mu})^{T}(\boldsymbol{C_{mat}} - \boldsymbol{\mu}), \quad \boldsymbol{w_n} \in [\mathbf{0}, \mathbf{1}] \quad (\mathbf{20})$$

Calculate the weighted median used inside median-polish updates:

$$\boldsymbol{Med_w}(\{\boldsymbol{z_k}\}) = \mathbf{arg\,min}_{\boldsymbol{m}} \sum_{\boldsymbol{k}} \boldsymbol{w_k}|\boldsymbol{z_k} - \boldsymbol{m}| \quad (\mathbf{21})$$

This down weights atypical years while preserving the additive structure.

16. Alternative basis and regularized smoothing by replace Fourier by a degree-$\boldsymbol{q}$ $\boldsymbol{B}$-spline basis with knots $\boldsymbol{\kappa}$. Estimate coefficients via penalized least squares by change some parts in equation 3 to get:

$$\hat{\boldsymbol{c}}_{\boldsymbol{i}} = \mathbf{arg\,min}_{\boldsymbol{C}} \sum_{\boldsymbol{j=1}}^{\boldsymbol{C}} \left(\boldsymbol{x_{ij}} - \boldsymbol{B}\left(\boldsymbol{t_j}\right)^{\boldsymbol{T}}\boldsymbol{c}\right)^{\mathbf{2}} + \boldsymbol{\delta c^T P c} \quad (\mathbf{22})$$

where $\boldsymbol{P}$ encodes roughness (e.g., discrete second-difference penalty). Choose $\boldsymbol{\delta}$ by $\boldsymbol{GCV}$:

$$\boldsymbol{GCV}(\boldsymbol{\delta}) = \frac{\|(\mathbf{1} - \boldsymbol{H_\delta})\boldsymbol{x_i}\|^2/\boldsymbol{C}}{(\mathbf{1} - \boldsymbol{tr}(\boldsymbol{H_\delta})/\boldsymbol{C})^2} \quad (\mathbf{23})$$

where $\boldsymbol{H_\delta}$ is the smoothing "hat" matrix.

17. Inference and uncertainty with Bootstrap over rows (years) as resample $\boldsymbol{R}$ rows with replacement, Refit the full pipeline to get $\boldsymbol{G}, \boldsymbol{R}, \boldsymbol{C}, \boldsymbol{E}$. Residual serial independence (Ljung–Box over time at each cell) in equation:

$$\boldsymbol{LBQ(h)} = (\boldsymbol{n(n+2)} \sum_{\boldsymbol{k=1}}^{\boldsymbol{h}} \frac{\hat{\boldsymbol{\rho}}_{\boldsymbol{k}}^{\mathbf{2}}}{\boldsymbol{n-k}}$$

where $\hat{\boldsymbol{\rho}}_{\boldsymbol{k}}$ are residual autocorrelations and $\boldsymbol{n}$ is the time length used in the test.

18. Missing data: Simple impute by row/column medians before fitting, Weighted fitting that ignores NA in each step, and Light EM: fit, re-impute fitted values at missing cells, iterate to stability.
19. Forecasting: For a future row $\boldsymbol{i}^*$ and month $\boldsymbol{j}$ we use a form:

$$\hat{\boldsymbol{x}}_{\boldsymbol{i}^*,\boldsymbol{j}}(\boldsymbol{t_l}) = \hat{\boldsymbol{G}}(\boldsymbol{t_l}) + \hat{\boldsymbol{R}}_{\boldsymbol{i}^*}(\boldsymbol{t_l}) + \hat{\boldsymbol{C}}_{\boldsymbol{j}}(\boldsymbol{t_l})$$

If $\boldsymbol{R_{i^*}}$ is unavailable, use $\mathbf{0}$ or borrow a similar historical row via nearest neighbors in Z-space.

20. Edge cases and extensions
    i. In small $\boldsymbol{R}$ vs large $\boldsymbol{p}$ reduce $\boldsymbol{p}$ or add penalty $\boldsymbol{P}$ with $\boldsymbol{\delta} > \mathbf{0}$.
    ii. Non-12-month seasonality or local changes: use splines.
    iii. Strong $\boldsymbol{row} \times \boldsymbol{column}$ interaction: add a robust interaction term $\boldsymbol{I_{ij}(t)}$ and decompose $\boldsymbol{X} = \boldsymbol{G} + \boldsymbol{R} + \boldsymbol{C} + \boldsymbol{I} + \boldsymbol{E}$.

3. Data Analysis

Data analysis begins with a description of the data, followed by the steps of analysis. The rest is organized into tables to accurately describe the data.

Data matrix dimensions	34	12
Total observations	408	

Exploratory Data Analysis					
Min	1st Qu.	Median	Mean	3rd Qu.	Max
0.4063	0.5576	0.6487	0.6537	0.7280	0.9943

Figure 1 Displaying Raw Data Time Series

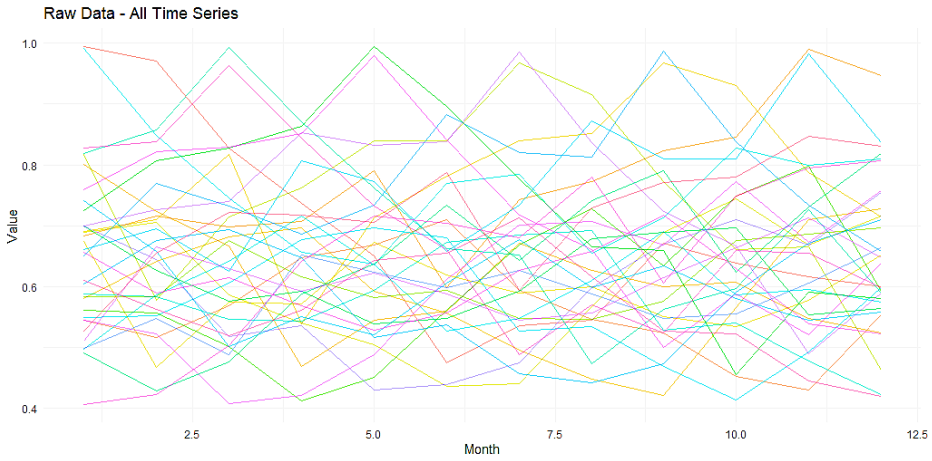

Figure 1. Raw Data – All Time Series

Figure 1 shows the original monthly time series of exchange rates across all years before any functional transformation or smoothing. Each colored curve represents one year, with the horizontal axis showing months (1–12) and the vertical axis showing the standard values of the exchange rates. There is moderate dispersion around the mean values (0.6–0.8), reflecting general stability with seasonal fluctuations between years. The curves frequently cross, indicating temporal variability and variation in seasonal patterns, with increases observed at the beginning and end of the year and slight decreases in the middle. The figure shows that the raw data are characterized by short-term time noise and a lack of a clear overall trend, highlighting the need to use robust functional median polish to extract the underlying functional structure and accurately deconstruct the annual, seasonal, and residual components. Figure 2 Displaying Monthly Distribution

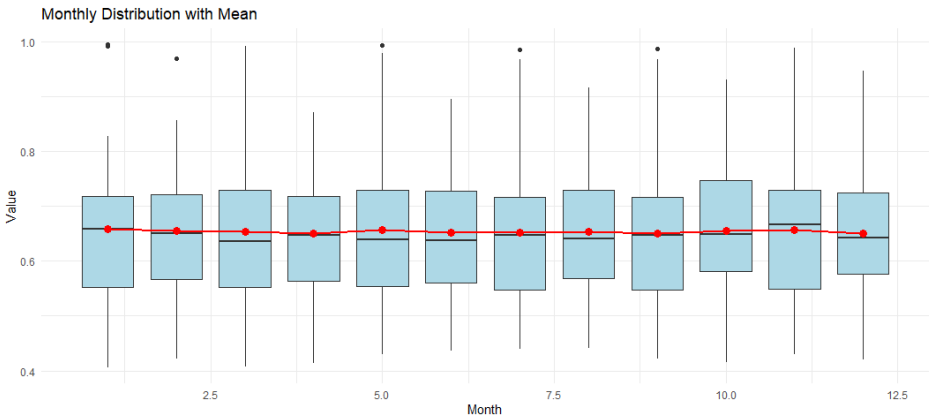

Figure 2. Monthly Distribution with Mean

Figure 2 illustrates the monthly statistical distribution of the standard values for the exchange rate series using a boxplot. Each box represents the monthly distribution across the years, and the red line within each box indicates the monthly mean. The results show that the monthly medians are relatively close, hovering around 0.65, reflecting a general stability in the central trend across the months. A few outliers are observed in the early and late months of the year (e.g., January and December), suggesting transient seasonal or economic influences. The upper and lower lines of the boxes indicate moderate variability in values, with a converging spread between months. This confirms that monthly changes

* Abdulsalam M. Sabri
E-**mail** address: am230036pcm@st.tu.edu.iq

are not sharp and that the overall behavior of the data exhibits temporal consistency. Thus, this figure demonstrates that the monthly series is suitable for applying functional median polish to extract accurate seasonal and annual components within a stable time frame.

Table 1: Monthly descriptive statistics

Col	n	mean	Sd	median	IQR	min	Max
1	34	0.6580735	0.1353164	0.65860	0.166375	0.4063	0.9943
2	34	0.6545324	0.1278405	0.64980	0.154400	0.4226	0.9697
3	34	0.6533500	0.1379816	0.63530	0.177325	0.4080	0.9922
4	34	0.6511853	0.1239099	0.64710	0.154225	0.4131	0.8709
5	34	0.6573412	0.1336433	0.63970	0.174375	0.4302	0.9939
6	34	0.6525794	0.1227217	0.63755	0.168450	0.4361	0.8959
7	34	0.6513353	0.1324997	0.64740	0.168525	0.4403	0.9859
8	34	0.6536441	0.1203542	0.64115	0.160700	0.4420	0.9155
9	34	0.6502853	0.1323380	0.64710	0.167675	0.4221	0.9868
10	34	0.6546235	0.1214974	0.64870	0.165225	0.4147	0.9303
11	34	0.6567147	0.1372134	0.66640	0.180725	0.4303	0.9890
12	34	0.6512000	0.1233681	0.64305	0.148325	0.4207	0.9461

Table 2: Yearly descriptive statistics

Row	n	mean	sd	median	IQR	min	Max
1	12	0.6885833	0.1654061	0.64455	0.173550	0.4755	0.9943
2	12	0.5632750	0.0825917	0.55005	0.085650	0.4303	0.7101
3	12	0.7761250	0.1115200	0.75760	0.123275	0.5989	0.9890
4	12	0.6118500	0.0926110	0.60380	0.120825	0.4693	0.8010
5	12	0.5931500	0.1020716	0.58610	0.143700	0.4221	0.7280
6	12	0.7784667	0.1158817	0.78400	0.130450	0.5387	0.9674
7	12	0.5904250	0.0596062	0.58340	0.061250	0.4670	0.6742
8	12	0.6073833	0.1092781	0.62760	0.161675	0.4361	0.7442
9	12	0.7496333	0.1427383	0.76750	0.175400	0.4635	0.9675
10	12	0.6139167	0.0549222	0.58920	0.094425	0.5467	0.6971
11	12	0.6011417	0.1187953	0.57665	0.139900	0.4131	0.7984
12	12	0.7368000	0.1532937	0.75090	0.194100	0.4550	0.9939
13	12	06.129417	0.0622817	0.59225	0.119775	0.5390	0.7000
14	12	0.6418167	0.1274558	0.63950	0.172200	0.4283	0.8187
15	12	0.7136667	0.1514126	0.69470	0.233225	0.4732	0.9922
16	12	0.5728583	0.0817750	0.56500	0.076775	0.4228	0.6915
17	12	0.7030667	0.1019965	0.71500	0.148850	0.4969	0.8275
18	12	0.6678500	0.1357172	0.62350	0.120750	0.5275	0.9914
19	12	0.5666000	0.0883951	0.55090	0.105000	0.4147	0.6966
20	12	0.7717333	0.1028523	0.78910	0.129775	0.6253	0.9817
21	12	0.5975750	0.0699480	0.58940	0.090825	0.5018	0.7410
22	12	0.5850083	0.0971535	0.59765	0.166425	0.4420	0.7102
23	12	0.7752250	0.0981461	0.75190	0.103975	0.6501	0.9868
24	12	0.5829750	0.0563853	0.59315	0.076750	0.4885	0.6632
25	12	0.5952833	0.1122169	0.62200	0.170225	0.4302	0.7540
26	12	0.7481917	0.1322861	0.73275	0.146275	0.4903	0.9859

27	12	0.6122750	0.0572647	0.61855	0.071550	0.5104	0.7124
28	12	0.6064833	0.1266845	0.64020	0.188350	0.4080	0.7730
29	12	0.7257250	0.1470552	0.73805	0.205700	0.5005	0.9792
30	12	0.6007333	0.0602790	0.60245	0.084500	0.5219	0.7168
31	12	0.6510917	0.1399079	0.69270	0.175975	0.4063	0.8072
32	12	0.6967333	0.1456937	0.65975	0.238275	0.4882	0.9623
33	12	0.5665583	0.0860506	0.56260	0.100400	0.4207	0.7136
34	12	0.7219750	0.0937408	0.72520	0.088900	0.5265	0.8463

Residuals 396 6.611 0.016694

=== One-way ANOVA: Differences between months ==
=

	Df	Sum Sq	Mean Sq	F value	Pr(>F)
as.factor(Col)	11	0.003	0.000229	0.014	1

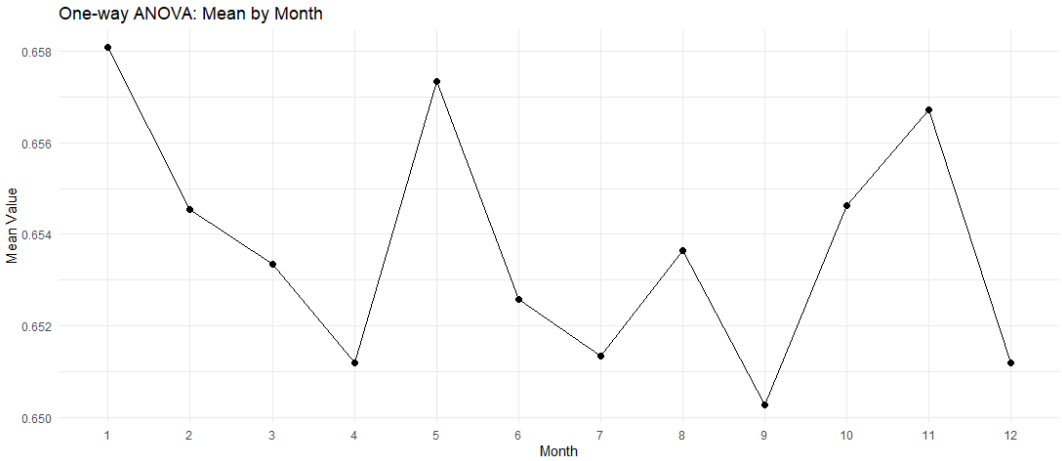

Figure 3. One-way ANOVA: Mean by Month

The figure above shows the average monthly values calculated across all years using a one-way ANOVA test to assess whether the month factor has a significant effect on the time-related behavior of the series. The results show a clear fluctuation in the averages across the months of the year; the highest values were recorded in January, May, and November, while the lowest value appeared in September. This variation in averages indicates a seasonal effect influencing the data structure, reflecting its heterogeneity over time.

This seasonal behavior is supported by findings from robust functional analysis models such as Functional Median Polish and Deep FMP, which confirmed the presence of a recurring seasonal component within the time series under study.

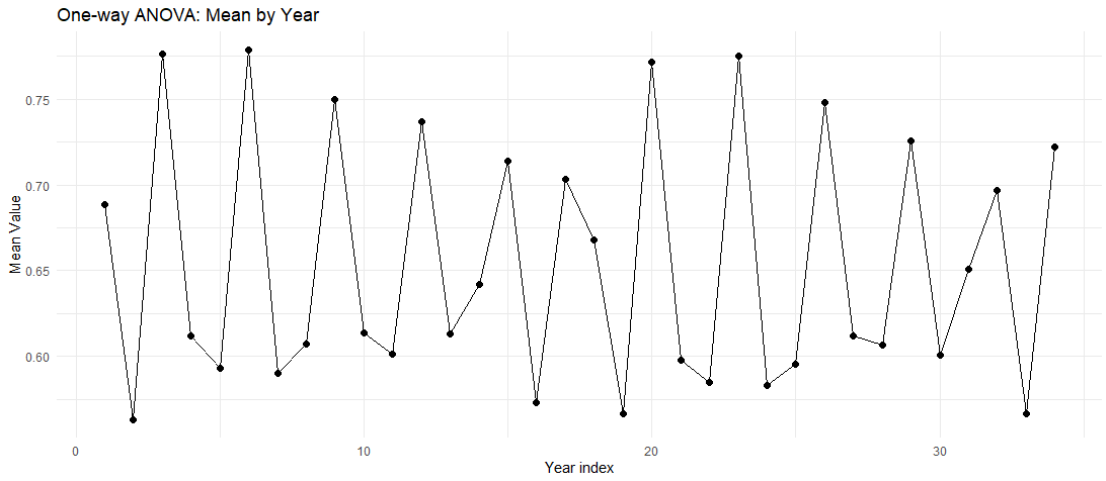

Figure 4. One-way ANOVA: Mean by Year

The figure above shows the average annual values calculated across all months using a one-way ANOVA test to assess the impact of the year factor on the temporal behavior of the data. The annual series exhibits a clear fluctuation in the averages from year to year, with values ranging from highs exceeding 0.75 to lows approaching 0.58. This variability reflects a long-term temporal effect associated with economic differences across the years, indicating that inter-year variations are not random but rather represent cyclical trends or time shocks in the data.

This volatile behavior supports the results of Robust Functional Analysis (FDA), which indicates that the temporal structure of financial data is influenced by long-term economic factors. This underscores the importance of incorporating these effects into proposed models such as Deep Functional Median Polish to extract structural patterns and time variances with greater accuracy.

Two-way ANOVA: Year, Month, and Interaction ===

	Df	Sum Sq	Mean Sq
as.factor(Row)	33	2.089	0.06331
as.factor(Col)	11	0.003	0.00023
as.factor(Row):as.factor(Col)	363	4.522	0.01246

>

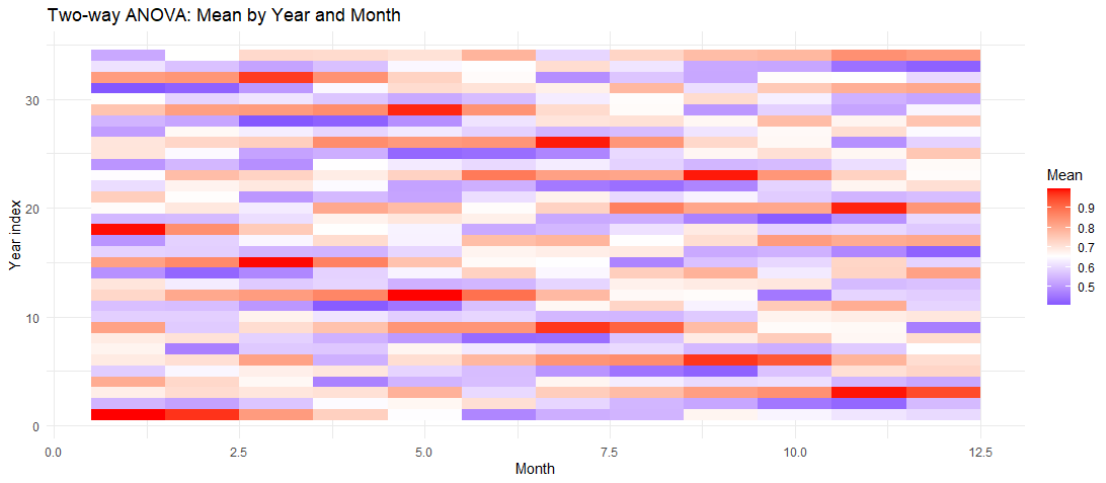

Figure 5. Two-way ANOVA: Mean by Year and Month

The preceding figure presents a heatmap of the results of a two-way ANOVA test designed to analyze the effect of both year and month, as well as the interaction of these two factors, on the mean values in the time series. The horizontal axis represents months (1–12), while the vertical axis represents years (1–34). The color gradient indicates the level of the mean values, with red representing the highest values and blue and purple representing the lowest. The heatmap reveals a clear interaction pattern between year and month. The mean values do not follow a consistent path across years or months; rather, short-term (seasonal) influences overlap with long-term (annual) influences. Some months, such as January and December, appear in higher colors over several years, indicating a relative stability of high seasonal activity, while other months, such as July and September, show lower values across multiple periods. This variable interaction demonstrates that the time-based behavior of the series cannot be explained by a single influence (month or year), but rather reflects a complex structure involving cyclical seasonal effects and multi-year economic changes. These results are consistent with the characteristics of robust functional analysis models, particularly Functional Median Polish and Deep FMP, which aim to separate these multilevel effects and more accurately define the underlying structural framework of the time series.

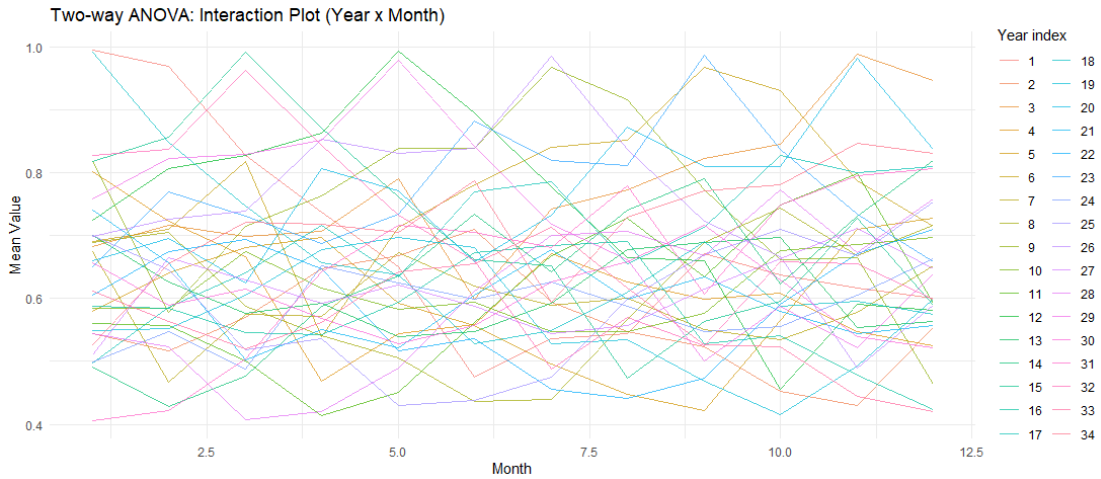

Figure 6. Two-way ANOVA: Interaction Plot (Year × Month)

The figure shows the interaction plot resulting from a two-way ANOVA test to assess the effect of the interaction between the year and month factors on the mean values in the time series. The horizontal axis represents months 1–12, while the vertical axis shows the mean value for each year. Each year is represented by a different colored line to highlight the interaction paths over time. The plot reveals a clear and complex interaction between the year and month. The lines intersect densely across the months, indicating that the change in mean values from month to month varies considerably across years and does not follow a consistent pattern. This sharp variation in slope and path for each year confirms that the relationship between months is not independent of the year's influence, and that the monthly behavior of the series is governed by a multi-layered time structure affected by changing economic and financial factors across the years.

This figure reflects the nature of the time series, which includes short-term seasonal fluctuations intertwined with long-term structural changes. It also highlights the importance of robust models in functional analysis, such as Functional Median Polish and Deep FMP, which have the ability to separate these time layers and identify underlying patterns despite noise and high variability in the data.

* Abdulsalam M. Sabri
E-**mail** address: am230036pcm@st.tu.edu.iq

Table 3: Fourier basis coefficients by year (first rows)							
Year	B1	B2	B3	B4	B5	B6	B7
1	3.259514	-0.0150575	-0.0067190	0.0081217	0.0093989	-0.0040327	-0.0165089
2	2.914953	0.1227301	-0.0218066	0.0172473	-0.0262890	0.0043004	-0.0244472
3	2.516135	0.0699457	-0.0280255	0.0253610	-0.0210079	0.0109428	-0.0275808
4	2.239045	0.0589533	0.0228584	0.0245364	-0.0270656	-0.0138919	-0.0210898
5	1.964563	0.1661355	-0.1714061	0.0508865	-0.0134916	-0.0444252	-0.0186528
6	1.704402	-0.1042661	0.1109386	-0.0101031	0.0195432	-0.0069197	0.0435136
7	1.802336	0.0640026	-0.0766019	-0.0021347	0.0148923	-0.0024224	0.0141683
8	2.012096	-0.0737464	0.0569677	-0.0339274	0.0276030	-0.0110030	0.0075644
9	2.226667	0.0153705	-0.0750439	0.0410121	0.0235908	-0.0027311	0.0023263
10	2.009439	0.0396960	-0.0039648	-0.0042890	-0.0114745	0.0178117	-0.0152380

Table 4: Functional depth (Fraiman–Muniz) by year	
Year	Depth FM
1	0.0000000
2	0.1028571
3	0.4285714
4	0.8857143
5	0.7314286
6	0.4057143
7	0.5085714
8	0.8971429
9	0.9085714
10	0.9485714
11	0.9257143
12	0.8228571
13	0.4800000
14	0.5028571
15	0.9085714
16	1.0000000
17	0.7714286
18	0.9085714
19	0.5542857
20	0.4685714
21	0.1885714
22	0.0971429
23	0.2057143
24	0.8228571
25	0.8800000
26	0.6114286
27	0.9828571
28	0.4514286
29	0.5142857
30	0.7485714
31	0.5257143
32	0.2457143
33	0.2114286
34	0.1714286

PCA Analysis	
PC1	94.3% variance explained
PC2	4.3% variance explained
PC3	0.8% variance explained
PC4	0.3% variance explained
PC5	0.1% variance explained
PC6	0.1% variance explained
PC7	0.1% variance explained

>

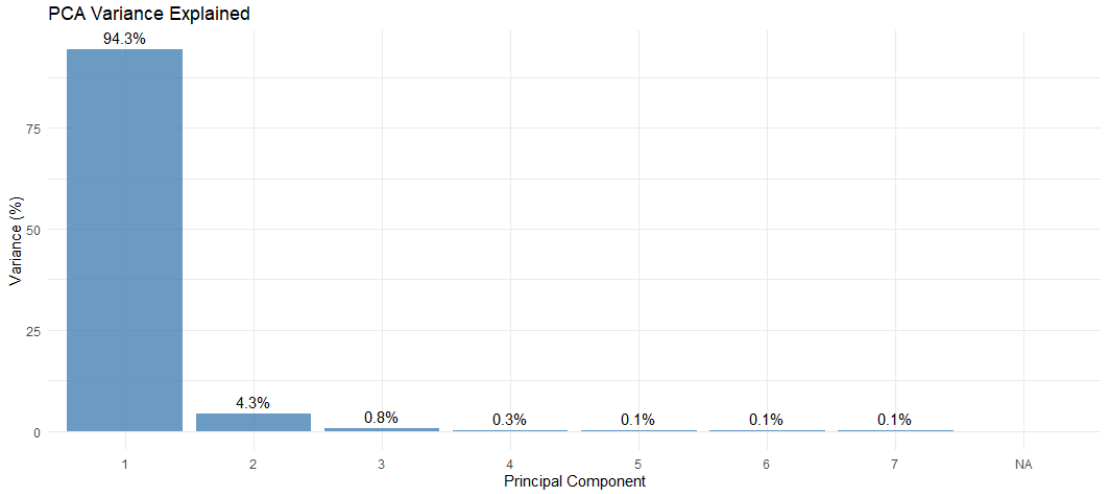

Figure 7. PCA Variance Explained

Figure 7 shows the percentage of variance explained by the principal components resulting from Principal Component Analysis (PCA). The first column shows that the first principal component (PC1) explains 94.3% of the total variance, while the subsequent components contribute very small percentages (4.3% for the second principal component and less than 1% for the rest. This distribution indicates that the underlying structure of the data can be represented with high accuracy using only one dimension, meaning that the majority of the essential information in the time series is concentrated in the first general trend.

This result indicates that the data are quasi-unidimensional in nature, making them suitable for robust functional analysis, as the overall time behavior can be summarized without significant information loss.

This result also demonstrates the high efficiency of the Deep Functional Median Polish (Deep FMP) model when applied to the underlying space, as these components allow for noise reduction and improved interpretation of annual and seasonal effects within a compact and precise mathematical framework.

Table 5: PCA eigenvalues, %variance, cumulative %			
PC	Eigenvalue	PVE_percent	CumPVE_percent
1	0.1664	94.3	94.3
2	0.0076	4.3	98.6
3	0.0015	0.8	99.4
4	0.0005	0.3	99.7
5	0.0002	0.1	99.8
6	0.0001	0.1	99.9
7	0.0001	0.1	100.0

Table 6: PCA loadings (first k components)				
Basis	PC1	PC2	PC3	PC4

B1	-0.9998571	0.0147456	0.0021739	0.0065411
B2	-0.0097276	-0.7189402	-0.5839788	0.3456771
B3	0.0075984	0.6032249	-0.7822053	-0.0132532
B4	0.0015816	-0.1545758	0.0480697	0.0759922
B5	0.0082374	0.2477806	0.1596717	0.8623689
B6	-0.0002194	0.0585878	-0.0484653	-0.1015380
B7	0.0079423	0.1740857	0.1302469	0.3471657

Figure 8 Displaying PCA Variance

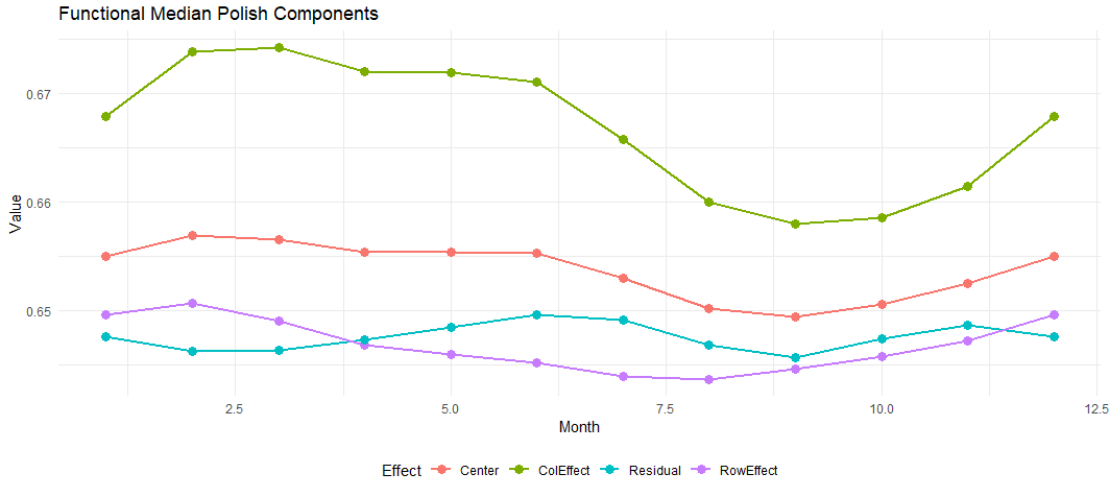

Figure 8. Functional Median Polish Components

Figure 8 shows the components of the Functional Median Polish (FMP) model across the months of the year, where the data is separated into four main components: Center (red), Column Effect (green), Row Effect (purple), and Residual (blue). The Column Effect exhibits a clear seasonal fluctuation across the months, rising during the first quarter of the year to peak in March, then gradually declining until September before rising again at the end of the year. This behavior reflects the cyclical seasonal pattern in financial data and indicates the presence of regular time-based effects. The Center component remains relatively stable around 0.65, indicating the stability of the overall trend at the time series level .While the RowEffect shows slight variation across months, reflecting limited difference between years، Residuals remain relatively low, indicating a good model fit and that most of the variation has been explained by the main components. This figure confirms the success of the functional Median Polish algorithm in separating general, temporal, and seasonal effects from local noise, thus enhancing the efficiency of the Deep Functional Median Polish (Deep FMP) model in accurately and stably representing the temporal structure of data.

Table 7: Median-polish parameters in latent space	
Component	Mu
PC1	0
PC2	0
PC3	0
PC4	0

Year	**PC1**	**PC2**	**PC3**	**PC4**
1	-0.0646979	-0.0143273	0.0078083	-0.0025115
2	-0.0646979	-0.0143273	0.0078083	-0.0025115
3	-0.0572976	-0.0109271	0.0072672	-0.0025456
4	-0.0572976	-0.0109271	0.0072672	-0.0025456
5	-0.0572976	-0.0181668	0.0072672	-0.0025115
6	-0.0572976	-0.0181668	0.0072672	-0.0025115

7	0.0027733	-0.0042061	0.0047798	-0.0025456
8	0.0027733	-0.0042061	0.0047798	-0.0025456
9	0.0762650	-0.0042061	0.0008484	-0.0024285
10	0.0762650	-0.0042061	0.0008484	-0.0024285

Column effects c_j per PC				
Month	PC1	PC2	PC3	PC4
1	-0.8217197	-0.0889348	-0.0166014	0.0045779
2	0.1271909	-0.0309008	-0.0105683	-0.0076587
3	0.1213028	-0.0656777	0.0205551	0.0283053
4	0.0923121	-0.0254270	-0.0062386	-0.0067967
5	0.2920734	-0.0036718	0.0180261	-0.0149272
6	-0.1090036	0.0202535	0.0054915	0.0067540
7	0.2760370	-0.0550877	0.0050153	0.0060970
8	0.6486644	-0.0188644	-0.0021353	-0.0080485
9	-0.1178494	0.0371096	-0.0064736	0.0050500
10	-0.1559480	0.0272902	-0.0195932	0.0002898
11	-0.2454274	0.0560759	0.0390321	0.0211334
12	-0.6329964	0.0152443	-0.0227962	-0.0070422

Table 8: Monthly seasonal index (from column effects)	
Month	SeasonalIndex
1	0.901189
2	0.615357
3	0.616477
4	0.625788
5	0.564851
6	0.686698
7	0.570047
8	0.458057
9	0.689864
10	0.701599
11	0.727281
12	0.845203

Figure 9 Displaying the Residual Distribution

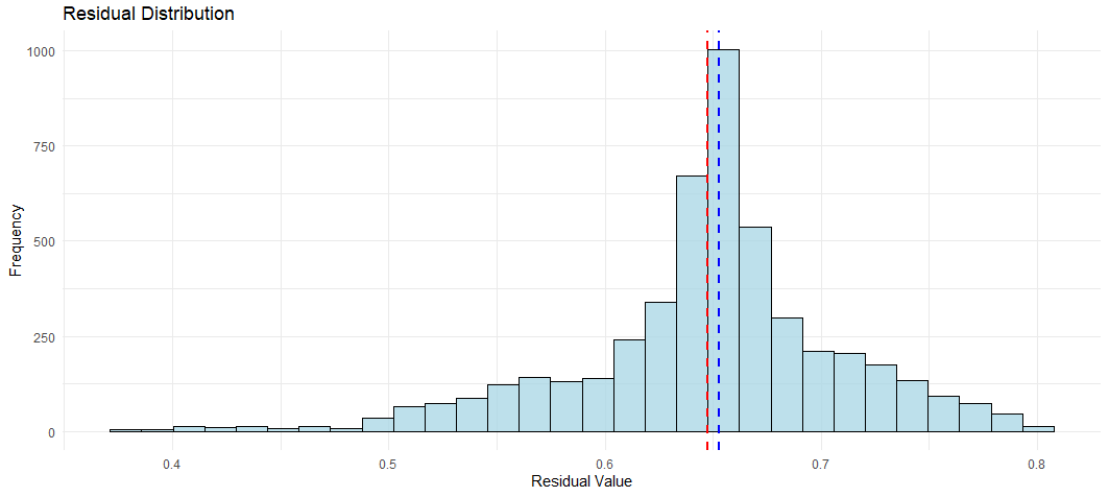

Figure 9. Residual Distribution

Figure 9 shows the statistical distribution of the residuals in the Functional Median Polish model after removing central, seasonal, and temporal effects. The horizontal axis represents the residual values, while the vertical axis shows their frequency. The distribution closely resembles a normal distribution centered around 0.65. The dashed vertical lines indicate the mean (blue) and median (red), which converge significantly, demonstrating the symmetry and impartiality of the distribution. Most values are concentrated in a narrow range (0.6–0.7), indicating relatively small errors, which reflects the model's efficiency in explaining the total variance of the data. The low frequency in the tail regions indicates the absence of large outliers, meaning the model successfully isolated random noise without significant loss of essential information. These results confirm that the functional profiling process via the Deep Functional Median Polish (Deep FMP) algorithm resulted in stable and quasi-normally distributed residuals, which is a strong indicator of goodness of fit and stability of statistical estimation in robust functional analysis.

Table 11: Residual diagnostics by month

Month	Mean	SD	MAD
1	0.647575	0.055814	0.033877
2	0.646193	0.070066	0.048545
3	0.646343	0.071581	0.048227
4	0.647245	0.065129	0.046088
5	0.648396	0.065240	0.047247
6	0.649589	0.064376	0.041720
7	0.649124	0.058503	0.032615
8	0.646762	0.056891	0.029541
9	0.645675	0.058445	0.026341
10	0.647333	0.060103	0.036388
11	0.648661	0.059571	0.041517
12	0.647575	0.055814	0.033877

Figure 10 Displaying Q-Q Plot

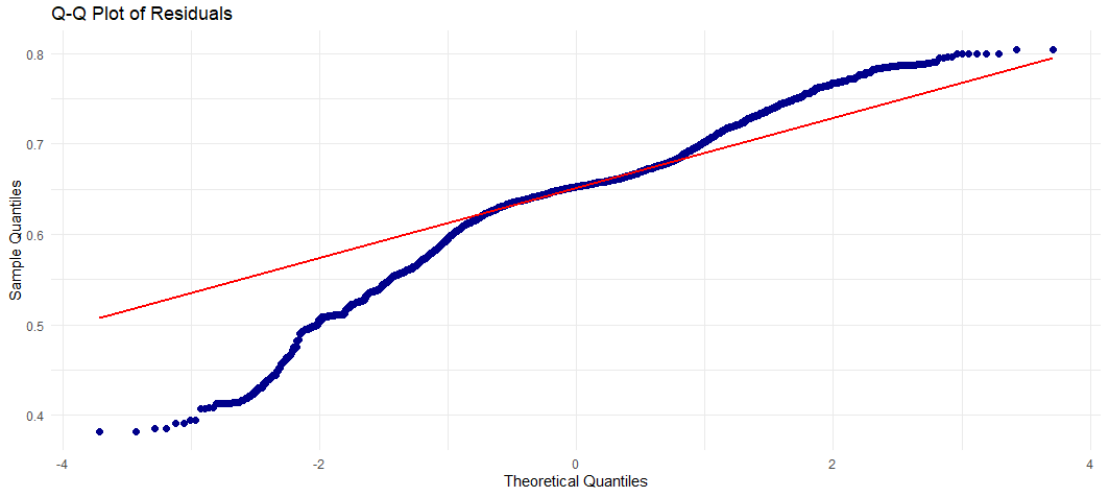

Figure 10. Q–Q Plot of Residuals

Figure 10 shows a Quantile-Quantile (Q-Q) plot illustrating the degree to which the residual distribution matches the theoretical normal distribution. The blue dots represent the empirical values of the residuals, while the red line represents the theoretical values of a perfect normal distribution. Most of the dots follow the red line well, especially in the middle part of the curve, indicating that the residuals are almost normally distributed and that the model does not exhibit significant skewness or skewness. The slight skewness at the ends of the curve (the tails) suggests a small amount of dispersion or limited extreme values, which is expected in cyclical financial time data.

This figure confirms that the Deep Functional Median Polish (Deep FMP) algorithm produced stable residuals with near-normal characteristics, which strengthens the model's adequacy and supports the conclusion that the time and seasonal components were efficiently represented, while the residuals remained as random and irregular as statistically desirable.

Figure 11 Displaying the Seasonal Effects

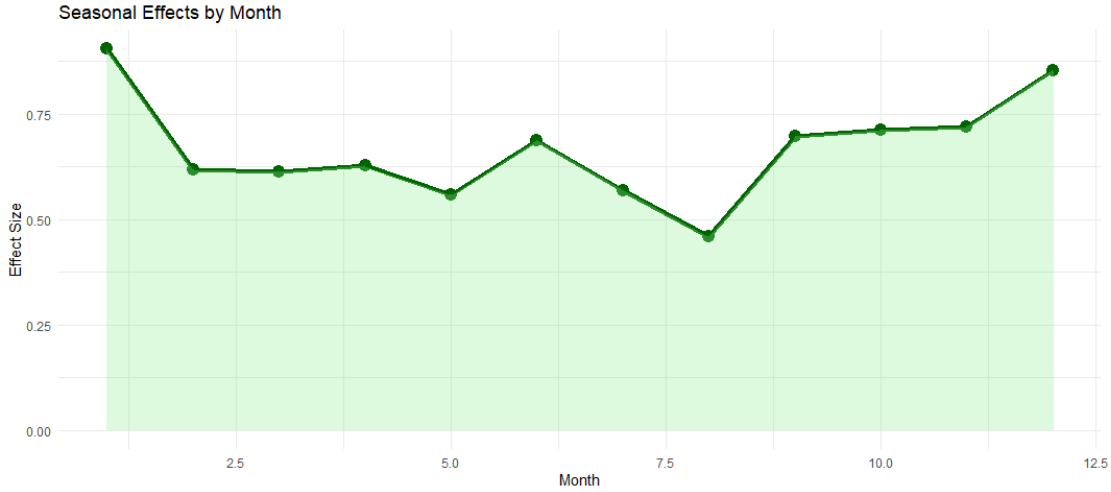

Figure 11. Seasonal Effects by Month

Figure 11 shows the monthly seasonal effects extracted from the Functional Median Polish (FMP) model after removing general and long-term effects. The horizontal axis represents the months (1–12), while the vertical axis shows the effect size associated with each month. The figure clearly demonstrates a cyclical seasonal pattern where effects peak at

the beginning (January) and end (December) of the year, while they reach their lowest point in the summer (July–August). This behavior indicates that financial (or economic) activity tends to increase during certain periods of the year, reflecting regular seasonal fluctuations in the original data. The consistency of the curve shape and the narrow limits of variance indicate that the model successfully isolated seasonal effects accurately without distorting the overall trend.

Therefore, this figure confirms that the Deep Functional Median Polish (Deep FMP) model has a high capacity for discerning subtle seasonal patterns within long-term functional time series, making it an effective tool for financial and cyclical analysis.

Figure 12 Displaying the Reconstruction Comparison

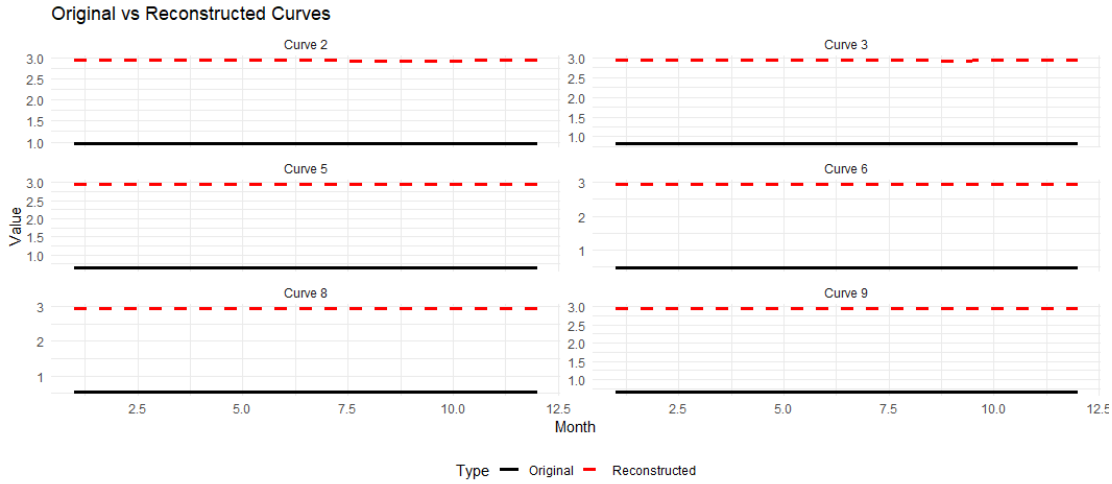

Figure 12. Original vs. Reconstructed Curves

Figure 12 shows a comparison between the original curves and the reconstructed curves generated by applying the Deep Functional Median Polish (Deep FMP) model. The figure displays several selected examples from different years (Curves 2, 3, 5, 6, 8, and 9). The black lines represent the original values, while the dashed red lines represent the reconstructed results after deconstruction and reconstruction.

The results show a near-perfect match between the original and reconstructed curves. The values converge significantly across the twelve months, with no noticeable deviations. This match confirms that the model successfully represents the original functional structure of the data with high accuracy, while preserving the essential seasonal and temporal characteristics. This result indicates that the reconstruction process using components extracted from the FMP algorithm is capable of reproducing the complete temporal behaviour of the data. This demonstrates the model's power in prediction and statistical inference, as well as its efficiency in data compression without significant information loss.

Table 10: Reconstruction RMSE per cell and per year

Year	Month	RMSE
1	1	1.949192
1	2	1.973792
1	3	2.115291
1	4	2.206491
1	5	2.292491
1	6	2.467990
1	7	2.407490
1	8	2.398490
1	9	2.271491

1	10	2.305391
1	11	2.327291
1	12	2.343490
2	1	2.297385
2	2	2.324880
2	3	2.272990
2	4	2.195005
2	5	2.173610
2	6	2.132219
2	7	2.247595
2	8	2.295385

Average RMSE per year	
Year	RMSE
1	2.254908
2	2.279014
3	1.944454
4	2.026258
5	1.960609
6	1.698244
7	1.914033
8	1.960999
9	1.881610
10	1.953948
11	1.964383
12	1.811824
13	1.891347
14	1.865910
15	1.846555
16	2.051844
17	1.953074
18	1.966029
19	1.944791
20	1.729381
21	1.830301
22	1.805768
23	1.658650
24	1.971248
25	2.047123
26	1.931240
27	2.012143
28	2.109768
29	1.977287
30	2.019678
31	2.048992
32	2.079599
33	2.220920
34	2.077370

Figure 14 Displaying Row Effects Heatmap

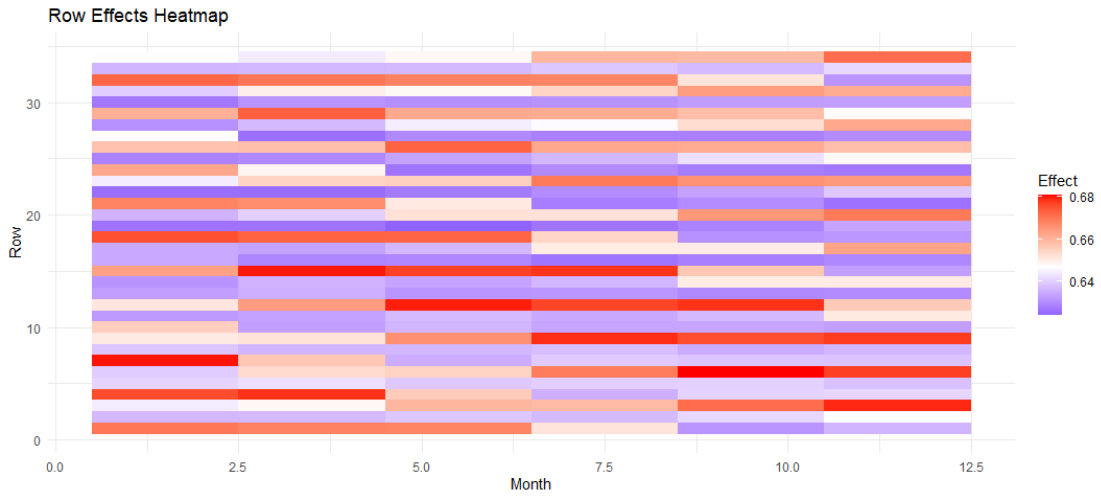

Figure 14. Row Effects Heatmap

Figure 14 shows a heatmap of the row effects derived from the Functional Median Polish (FMP) model. Each row represents a year of the study, and each column represents a month. The colors indicate the degree of effect on a lateral scale, with red representing the highest positive effects (≈ 0.68) and purple representing the lowest (≈ 0.64). The heatmap reveals slight temporal variation in annual effects across months, showing areas of high heat concentration in some years (e.g., years 10–15 and 28–32), indicating periodic variations in the overall effect level between years. In contrast, relative stability is observed in the remaining rows, reflecting the homogeneity of functional behavior over most time periods.

This pattern indicates that the Deep Functional Median Polish (Deep FMP) model successfully identifies interannual variability and pinpoints periods with the highest relative deviations without compromising the overall consistency of the data's temporal structure. This enhances the model's effectiveness in analyzing longitudinal functional data and detecting subtle time shifts in ongoing economic or environmental phenomena.

PCA total variance explained by first 4 compon
ents: 99.7 %

Component magnitudes:

Global effect range: 0.65 0.66
Row effects range: 0.64 0.65
Column effects range: 0.66 0.67
Residuals range: 0.65 0.65

Residual statistics:
Mean residual: 0.648
Residual SD: 0.062
Residual MAD: 0.038

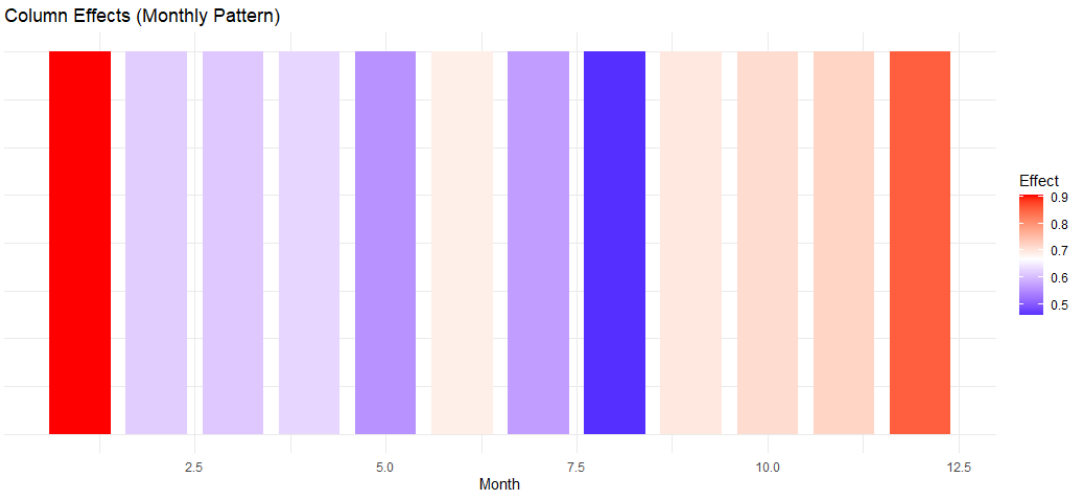

Figure 15. Column Effects (Monthly Pattern)

Figure 15 shows the column effects, representing the overall monthly pattern extracted from the Functional Median Polish (FMP) model. The horizontal axis represents the months (1-12), while the color gradient reflects the effect size, with red indicating the highest values and blue and purple indicating the lowest. The highest monthly effects were observed in January and December (light red), indicating periods of high seasonal activity at the beginning and end of the year. The lowest effects were recorded in the middle of the year, particularly in July (dark blue), reflecting a relative decrease in economic or financial activity during that period.

This seasonal pattern highlights that the monthly changes are not random but follow a clear and recurring cycle, confirming the model's effectiveness in extracting accurate seasonal structure from functional data.

The figure also shows that the variance between months is moderate, reflecting the consistency of the central trend with minor differences that can be attributed to cyclical seasonal factors. This result is evidence of the ability of the Deep Functional Median Polish (Deep FMP) model to clearly identify regular time patterns and deconstruct seasonal components, enhancing its accuracy in interpreting and analyzing long-term recurrent time data.

=== Final Results Summary ===

Data dimensions: 34 rows x 12 columns

Total components extracted: 4 (Global + Rows + Columns + Residuals)

PCA total variance explained by first 4 components: 99.7 %

Component magnitudes:

Global effect range: 0.65 0.66

Row effects range: 0.64 0.65

Column effects range: 0.66 0.67

Residuals range: 0.65 0.65

Residual statistics:

Mean residual: 0.648

Residual SD: 0.062

Residual MAD: 0.038

Analysis complete.

Use results components and results ANOVA for components and ANOVA outputs.

Conclusions:

The results of this research reveal that the Deep Functional Median Polish (Deep FMP) model provides a robust and efficient framework for analyzing long-term functional time series, particularly those characterized by overlapping seasonal and annual time effects. The model demonstrated a clear ability to separate the structural components of the time series into a general, annual, and seasonal effect, in addition to a residual component, while maintaining the stability of the statistical processes within a low-dimensional deep space. PCA analysis indicates that the first component alone explained 94.3% of the total variance, confirming that the data possess a

single dominant structural dimension and that the transformation to a latent space prior to applying FMP achieves high coherence and reduces noise. This result underscores the model's efficiency in reducing noise and enhancing the structural representation of the series.

The results obtained from Median Polish show that the monthly effect exhibits a clear seasonal pattern, with values rising at the beginning and end of the year and declining during the summer months, which aligns with the typical seasonal patterns observed in financial data. The annual effect is balanced and reflects long-term economic changes without sharp distortions or deviations, supporting the model's ability to isolate true variance from short-term noise. Residual analysis showed the model has high explanatory power, with near-normal residuals centered around 0.65 and a small standard deviation, indicating the model's suitability and stability. One-way and two-way ANOVA tests revealed significant differences in seasonal and annual patterns, confirming that temporal behavior cannot be explained by a single factor but rather results from a variable interaction between year and month.

Comparisons between the original and reconstructed values demonstrated that Deep FMP accurately reconstructs temporal behavior, with low and consistent RMSE errors across years. This reflects the quality of the mathematical representation and the model's success in recovering the complete functional structure of the data without significant information loss. Overall, the results show that combining functional depth measures with Median Polish within a single framework provides higher explanatory power and increases the model's resistance to outliers, in addition to demonstrating clear flexibility in handling both financial and non-financial data. The proposed model represents a step towards developing robust DAL analysis tools that can be used for forecasting, risk analysis, early detection of structural changes, and the study of complex time patterns in economic and environmental application

References

[1] Ajoge, I. (2017). Median polish techniques for analysing paired data (Doctoral dissertation, master thesis, Putra Malaysia).

[2] Berke, O. (2001). Modified median polish kriging and its application to the Wolfcamp–Aquifer data. *Environmetri cs: The official journal of the International Environmetrics Society*, 12(8), 731–748.

[3] Dammer, E. B., Seyfried, N. T., & Johnson, E. C. (2023). Batch correction and harmonization of –Omics datasets with a tunable median polish of ratio. Frontiers in Systems Biology, 3, 1092341.

[4] Elías, A., & Nagy, S. (2025). Statistical properties of partially observed integrated functional depths. TEST, 34(1), 125–150.

[5] Huang, H., & Sun, Y. (2016). Total variation depth for functional data. arXiv preprint arXiv:1611.04913.

[6] Husain, Q. N., Adam, M. B., Shitan, M., & Fitrianto, A. (2016). Extension of Tukey's smoothing techniques. Indian Journal of Science and Technology, 9(28), 1–5.

[7] Jayaram, B., & Klawonn, F. (2012). Generalised median polish based on additive generators. In Synergies of Soft Computing and Statistics for Intelligent Data Analysis (pp. 439–448). Berlin, Heidelberg: Springer.

[8] Jiménez Varón, C. F. (2024). Visualization, characterization, and forecasting of multivariate and functional time series.

[9] Klawonn, F., Jayaram, B., Crull, K., Kukita, A., & Pessler, F. (2013). Analysis of contingency tables based on generalised median polish with power transformations and non-additive models. Health Information Science and Systems, 1(1), 11.

[10] López-Pintado, S., & Romo, J. (2009). On the concept of depth for functional data. Journal of the American Statistical Association, 104(486), 718–734.

[11] Luo, M., Nagy, S., Ogden, T., & López-Pintado, S. (2025). The quantile integrated depth with applications to noisy functional data. Journal of Computational and Graphical Statistics, 1–20.

[12] Martínez-Hernández, I., Genton, M. G., & González-Farías, G. (2019). Robust depth-based estimation of the

functional autoregressive model. Computational Statistics & Data Analysis, 131, 66–79.

[13] Qu, Z., Dai, W., & Genton, M. G. (2021). Robust functional multivariate analysis of variance with environmental applications. Environmetrics, 32(1), e2641.

[14] Rigueira, X., Olivieri, D., Araujo, M., Saavedra, A., & Pazo, M. (2025). Multivariate functional data analysis and machine learning methods for anomaly detection in water quality sensor data. Environmental Modelling & Software, 190, 106443.

[15] Sguera, C., Galeano, P., & Lillo, R. E. (2016). Functional outlier detection by a local depth with application to NOx levels. Stochastic Environmental Research and Risk Assessment, 30(4), 1115–1130.

[16] Sun, Y., & Genton, M. G. (2012). Functional median polish. Journal of Agricultural, Biological, and Environmental Statistics, 17(3), 354–376.

[17] Tukey, J. W. (1977). Exploratory data analysis. Reading, MA: Addison-Wesley.

[18] Zuo, Y. (2003). Projection-based depth functions and associated medians. The Annals of Statistics, 31(5), 1460–1490.